Fisher information of a squeezed-state interferometer with a finite photon-number resolution

P. Liu,[1] P. Wang,[2] W. Yang,[2,*] G. R. Jin,[1,†] and C. P. Sun[2,‡]

[1]*Department of Physics, Beijing Jiaotong University, Beijing 100044, China*
[2]*Beijing Computational Science Research Center, Beijing 100084, China*

Squeezed-state interferometry plays an important role in quantum-enhanced optical phase estimation, as it allows the estimation precision to be improved up to the Heisenberg limit by using ideal photon-number-resolving detectors at the output ports. Here we show that for each individual N-photon component of the phase-matched coherent $\otimes$ squeezed vacuum input state, the classical Fisher information always saturates the quantum Fisher information. Moreover, the total Fisher information is the sum of the contributions from each individual N-photon component, where the largest N is limited by the finite number resolution of available photon counters. Based on this observation, we provide an approximate analytical formula that quantifies the amount of lost information due to the finite photon number resolution; e.g., given the mean photon number $\bar{n}$ in the input state, over 96% of the Heisenberg limit can be achieved with the number resolution larger than $5\bar{n}$.

I. INTRODUCTION

Quantum-enhanced optical phase estimation through a Mach-Zehnder interferometer (MZI) is important for multiple areas of scientific research [1–7], such as imaging, sensing, and high-precision gravitational waves detection. The MZI-based optical phase estimation consists of three steps [see, e.g., Fig. 1(a)]. First, a two-mode input state of the light is prepared. Second, the light passes successively through a beam splitter, the unknown relative phase shift φ between the two arms of the MZI, and another beam splitter, and it evolves to the output state. Third, the output state is measured for many times, and the outcomes $\mathbf{x} = \{x_1, x_2, \ldots, x_v\}$ are processed to construct an unbiased estimator $\hat{\varphi}(\mathbf{x})$ to the unknown parameter φ [8,9]. The estimation precision is quantified by the standard deviation $\Delta\varphi \equiv \sqrt{\langle(\hat{\varphi}(\mathbf{x}) - \varphi)^2\rangle}$. By using optimal data-processing techniques to extract all the information contained in the data, the estimation precision from $v \gg 1$ repeated measurements is given by the Cramér-Rao lower bound [8,9]: $\Delta\varphi_{\mathrm{CRB}} \equiv 1/\sqrt{vF(\varphi)}$, where $F(\varphi)$ is the classical Fisher information (CFI) for the measurement scheme used. Given the input state, maximizing $F(\varphi)$ over all possible measurement schemes gives the quantum Fisher information (QFI) F_Q and hence the quantum Cramér-Rao bound $\Delta\varphi_{\mathrm{QCRB}} \equiv 1/\sqrt{vF_Q}$ [10–14], which sets an ultimate precision for estimating the unknown phase shift φ. Usually the precision $\Delta\varphi_{\mathrm{QCRB}}$ improves with increasing number of photons $\bar{n}$ contained in the input state. Using a coherent-state of light as the input, the achievable phase sensitivity per measurement is limited by the classical (or shot noise) limit $\delta\varphi \equiv \sqrt{v}\Delta\varphi \sim 1/\sqrt{\bar{n}}$, as the QFI $F_Q \sim O(\bar{n})$.

To improve the precision beyond the classical limit ($\sim 1/\sqrt{\bar{n}}$), it is necessary to employ quantum resources, such as entanglement and squeezing in the input state [1–7]. In this context, the squeezed states of light play an important role and have been widely studied in the past few decades ever since

the pioneer work of Caves [1], who showed that by feeding a coherent state $|\alpha\rangle$ into one port of the MZI and a squeezed vacuum $|\xi\rangle$ into the other port, the unknown phase shift can be estimated with a precision beyond the classical limit. Pezzé and Smerzi [15] further suggested that the previously used phase estimator based on the averaged relative photon number is not optimal. When the injected fields are phase matched, i.e., the phases of two light fields θ_a and θ_b obeying $\cos(\theta_b - 2\theta_a) = +1$, the QFI can reach the Heisenberg scaling $\sim O(\bar{n}^2)$ for a given mean photon number $\bar{n} = |\alpha|^2 + \sinh^2|\xi|$. More importantly, this QFI can be saturated by the CFI for ideal photon counting measurements. Consequently, by using the optimal data-processing technique (such as the maximum-likelihood estimation or Bayesian estimation) to process these measurement outcomes, the phase estimation precision can attain the Heisenberg limit $\delta\varphi_{\mathrm{CRB}} = \delta\varphi_{\mathrm{QCRB}} \sim 1/\bar{n}$. Recently, Lang and Caves [16] proved that given the total average photon number $\bar{n}$ of the input state, if a coherent light is fed into one input port of the MZI, then the squeezed vacuum is the optimal state to inject into the second input port. Liu *et al.* [17] have analyzed the phase-matching condition (PMC) that maximizes the QFI in the squeezed-state interferometer, where a superposition of an even or odd number of photons is injected from one port of the interferometer and any input state from another.

An important requirement of these theoretical works [15,16] is to take into account all the photon-counting events, which in turn requires photon-number-resolving detectors with perfect number resolution [18]. However, on the experimental side, the best detector to date can resolve the number of photons only up to four [19,20]. This makes it unclear whether or not the Heisenberg limit of the estimation precision can still be achieved by using realistic photon detectors with an upper threshold on the number resolution. To bridge this gap between the theory and experiments, it is of interest to investigate the experimentally achievable estimation precision when the total number of photons being detected is limited, i.e., $N = N_1 + N_2 \leqslant N_{\mathrm{res}}$, where $N_{\mathrm{res}}/2$ determines the number resolution by a single photon-counting detector. Since the existence of an upper threshold N_{res} essentially amounts to discarding the information contained in photon-counting

————
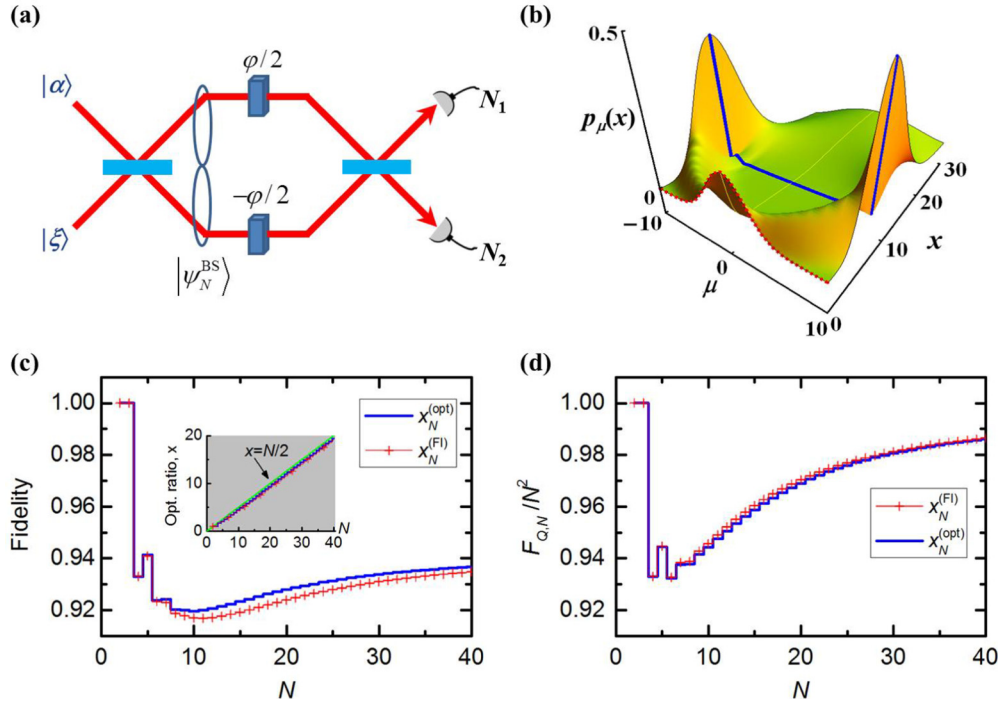*wenyang@csrc.ac.cn
†grjin@bjtu.edu.cn
‡cpsun@csrc.ac.cn

FIG. 1. (a) Photon-counting measurement at output ports of the MZI fed with a coherent state $|\alpha\rangle$ and a squeezed vacuum $|\xi\rangle$, and the N-photon state $|\psi_N^{\text{BS}}\rangle$, postselected by the number of photons being detected $N = N_1 + N_2 = 2J$. (b) For a given $J = N/2 = 10$, the probability distribution $p_\mu = |\langle J, \mu|\psi_N^{\text{BS}}\rangle|^2$ against $\mu = (N_1 - N_2)/2 \in [-J, +J]$ and $x = |\alpha|^2/\tanh|\xi|$. At a certain value of the ratio $x_N^{(\text{opt})}$ (blue line), the distribution shows two symmetric peaks at $\mu = \pm J$, indicating the appearance of a path-entangled NOON state. (c) The fidelity between the N-photon state and an ideal NOON state and (d) the QFI of the N-photon state, with their values calculated at $x = x_N^{(\text{opt})}$ (blue solid line) and $x_N^{(\text{FI})}$ (red line with crosses); see text. The inset in (c) indicates $x_N^{(\text{FI})} \leqslant x_N^{(\text{opt})} \leqslant N/2$.

events with the number of photons larger than N_{res}, it is therefore important to investigate the distribution of the QFI and CFI in the N-photon components of the coherent $\otimes$ squeezed vacuum input state and calculate how much the QFI is kept with a finite number resolution.

In addition, studying the distribution of the QFI and CFI in the N-photon components also helps to understand the phase estimation precision in recent postselection experiments. When the MZI is fed by the coherent $\otimes$ squeezed vacuum, the state after the first beam splitter of the MZI contains a small fraction of the path-entangled NOON state [21,22], which is a well-known N-photon nonclassical state that allows the phase estimation precision to achieve the Heisenberg limit [23–29]. In the limit $|\alpha|^2, |\xi| \ll 1$, Afek *et al.* [22] have demonstrated N-fold oscillations of the coincidence rates for N up to 5, manifesting the appearance of N-photon NOON states. However, the generation probability of a N-photon NOON state decreases dramatically with increasing N, e.g., the five-photon count rate ~ 3 per 100 s [22]. Therefore, it is desirable to study the overall estimation precision when such small generation probabilities are included, since there are general conclusions that the generated state under postselection cannot improve the precision for estimating a single parameter when the *total* number of input photons are included (see, e.g., Refs. [30–32]).

In this paper, we investigate the distribution of the QFI and CFI in the different N-photon components of the coherent $\otimes$ squeezed vacuum input state and provide the achievable estimation precision by using imperfect photon counters with

an upper threshold N_{res} for the photon number resolution. Under the PMC $\cos(\theta_b - 2\theta_a) = +1$, we show that the CFI always saturates the QFI for each *individual N*-photon component. Consequently, when the detectable number of photons is upper bounded by N_{res}, the phase estimation precision $\delta\varphi_{\text{CRB}}$ is always equal to $\delta\varphi_{\text{QCRB}}$ and both of them are determined by the sum of the CFI or equivalently the QFI for each N-photon component with N up to N_{res}. For the commonly used optimal input state with $|\alpha|^2 \simeq \sinh^2 |\xi| \simeq \bar{n}/2$ [15–17], photon-counting measurement with ideal photon detectors ($N_{\text{res}} \to \infty$) gives the CFI or the QFI $F_{Q,\text{opt}}^{(\text{id})} \sim \bar{n}^2$, leading to the Heisenberg limit of the estimation precision [15–17]. For finite photon number resolution, we provide an approximate analytical expression that quantifies the amount of lost information, which predicts that over 96% of the ideal QFI can be achieved as long as $N_{\text{res}} \gtrsim 5\bar{n}$. Compared with the ideal case (i.e., $|\alpha|^2 \simeq \sinh^2 |\xi|$), we find that the optimal input state contains more coherent light photons than that of the squeezed light.

II. FINITE N-PHOTON STATE UNDER POSTSELECTION

As illustrated schematically by Fig. 1(a), a postselection scheme for creating path-entangled NOON states has been proposed by injecting a coherent state of light and a squeezed vacuum into a Mach-Zehnder interferometer [21,22]. This scheme has been demonstrated by Afek *et al.* [22] in the limit $|\alpha|^2, |\xi| \ll 1$. However, the generated N-photon state in postselection cannot improve the precision for estimating

an unknown phase shift, since the CFI is weighted by the generation probability [30]. It is therefore important to investigate whether or not a sum of each N-component for N up to a finite number can beat the shot-noise scaling $\sim O(\bar{n})$. To answer this question, in this section we first derive explicit form of the N-photon state generated by postselection. Next, we calculate the (quantum) Fisher information for the N-photon state, which determines the ultimate precision on the phase estimation.

A. The fidelity of the N-photon state and the NOON state

Without any loss and additional reference beams, the input state can be expressed as a superposition of N-photon states [14], i.e., $|\alpha\rangle_a \otimes |\xi\rangle_b = \sum_N \sqrt{G_N}|\psi_N\rangle$, where G_N denotes the generation probability of a finite N-photon state, and $N = N_1 + N_2$ is the number of photons postselected by the photon-counting events $\{N_1, N_2\}$. In Fock basis, the N-photon state is given by

$$|\psi_N\rangle = \frac{1}{\sqrt{G_N}} \sum_{k=0}^{[N/2]} c_{N-2k}(\theta_a) s_{2k}(\theta_b)|N-2k, 2k\rangle_{a,b}, \quad (1)$$

where $|m,n\rangle_{a,b} \equiv |m\rangle_a \otimes |n\rangle_b$, and the sum over k is up to $[N/2] = (N-1)/2$ (for odd N), or $N/2$ (for even N), because of an even number of photons that injected from the port b. Note that the probability amplitudes of the coherent state and the squeezed vacuum $c_m(\theta_a) = \langle m|\alpha\rangle$ and $s_n(\theta_b) = \langle n|\xi\rangle$ depend explicitly on the phases of two input light fields θ_a and θ_b (see Appendix A). Furthermore, the generation probability G_N is also the normalization factor and is given by

$$G_N = \sum_{k=0}^{[N/2]} |c_{N-2k}s_{2k}|^2 = \frac{e^{-|\alpha|^2}}{\cosh|\xi|}\left(\frac{\tanh|\xi|}{2}\right)^N R_N(x), \quad (2)$$

where we have introduced a ratio $x \equiv |\alpha|^2/\tanh|\xi|$ and a polynomial

$$R_N(x) = \sum_{k=0}^{[N/2]} \frac{(2k)!}{(N-2k)!(k!)^2}(2x)^{N-2k}, \quad (3)$$

which obeys $R_N(0) = N!/[(N/2)!]^2$ for even N, and $R_N(0) = 0$ for odd N, similar to the Hermite polynomials at $x = 0$. In the limit $|\alpha|^2, |\xi| \ll 1$, the ratio can be approximated as $x \sim |\alpha|^2/|\xi|$, and its square is indeed the two-photon probability of the coherent state divided by that of the squeezed vacuum [22].

The explicit form of the N-photon state crucially depends on the relative phase difference between the squeezing parameter ξ and the coherent-state amplitude α. Following Refs. [15,17], we consider the PMC, i.e., $\cos(\theta_b - 2\theta_a) = +1$, for which Eq. (1) can be reexpressed as $|\psi_N\rangle = \exp(iN\theta_a)|\tilde{\psi}_N\rangle$, where $|\tilde{\psi}_N\rangle$ denotes the N-photon states with real amplitudes (for details, see Appendix A). After the first beam splitter, the N-photon state becomes

$$\left|\psi_N^{\mathrm{BS}}\right\rangle = e^{-i\pi J_x/2}|\psi_N\rangle = \sum_{\mu=-J}^{+J} \langle J,\mu|\psi_N^{\mathrm{BS}}\rangle|J,\mu\rangle, \quad (4)$$

where, for brevity, we have introduced the eigenstates of J_z, i.e., $|J,\mu\rangle \equiv |J+\mu, J-\mu\rangle_{a,b}$, with $J = N/2$ and

$\mu \in [-J, +J]$. Under the PMC, the probability amplitudes of $|\psi_N^{\mathrm{BS}}\rangle$ can be written as

$$\langle J,\mu|\psi_N^{\mathrm{BS}}\rangle = e^{iN\theta_a} e^{i\pi(\mu-J)/2}\sqrt{p_\mu}, \quad (5)$$

which depends solely on the phase of the coherent-state light θ_a and the probability distribution (see Appendix A)

$$p_\mu \equiv \left|\langle J,\mu|\psi_N^{\mathrm{BS}}\rangle\right|^2$$

$$= \frac{1}{R_N(x)}\left[\sum_{k=0}^{[N/2]} d_{\mu, J-2k}^J\left(\frac{\pi}{2}\right)\frac{\sqrt{(2k)!}}{k!\sqrt{(N-2k)!}}(2x)^{N/2-k}\right]^2, \quad (6)$$

where $d_{\mu,v}^J(\varphi)$ are the elements of Wigner's d-matrix [33,34]. It is interesting to note that for a given N, the probability distribution depends only on the introduced ratio $x = |\alpha|^2/\tanh|\xi|$, hereinafter denoted by $p_\mu = p_\mu(x)$.

Figure 1(b) shows the probability distribution as a function of μ for a large enough N. At $x = 0$, i.e., a pure squeezed vacuum being injected, the probability distribution is almost a Gaussian, due to $p_\mu(0) = [d_{\mu,-J}^J(\pi/2)]^2 \propto \exp(-\mu^2/J)$. As x increases, the N-photon state always shows a symmetric probability distribution (i.e., $p_{-\mu} = p_{+\mu}$). One can see this directly from Eq. (6), where $d_{-\mu,v}^J(\varphi) = (-1)^{J-v} d_{+\mu,v}^J(\pi - \varphi)$; see, e.g., Refs. [33,34]. Physically, the symmetric probability distribution arises from the fact that the N-photon state $|\psi_N\rangle$ contains only an even number of photons in mode b, i.e., $\langle\psi_N|J_y|\psi_N\rangle = \mathrm{Im}\langle\psi_N|a^\dagger b|\psi_N\rangle = 0$, which in turn leads to

$$\langle\psi_N|J_y|\psi_N\rangle = \langle\psi_N^{\mathrm{BS}}|J_z|\psi_N^{\mathrm{BS}}\rangle = \sum_{\mu\geqslant 0}(p_{+\mu} - p_{-\mu})\mu = 0 \quad (7)$$

and hence $p_{-\mu} = p_{+\mu}$. This symmetry enables us to write an explicit expression of the N-photon state,

$$\left|\psi_N^{\mathrm{BS}}\right\rangle = e^{iN\theta_a}\sum_{\mu\geqslant 0} e^{i\frac{\pi}{2}(\mu-J)}\sqrt{2p_\mu(x)}$$

$$\times \left(\frac{|J,\mu\rangle + e^{-i\pi\mu}|J,-\mu\rangle}{\sqrt{2}}\right), \quad (8)$$

which is indeed a superposition of the path-entangled states $\sim(|J,\mu\rangle + e^{-i\pi\mu}|J,-\mu\rangle)$, where the relative phase $e^{-i\pi\mu}$ comes from Eq. (5). For a certain value of x, the probability distribution $p_\mu(x)$ reaches its maximum at $\mu = \pm J = \pm N/2$, indicating $|\psi_N^{\mathrm{BS}}\rangle \rightarrow |\psi_{\mathrm{NOON}}\rangle = (|J,+J\rangle + e^{-i\pi J}|J,-J\rangle)/\sqrt{2}$, with the fidelity given by

$$\mathcal{F}_{\mathrm{NOON}} \equiv \left|\langle\psi_{\mathrm{NOON}}|\psi_N^{\mathrm{BS}}\rangle\right|^2 = 2p_J(x). \quad (9)$$

Clearly, the fidelity depends on the ratio x and the number of photons being detected N ($= 2J$). For a given N, maximizing the fidelity with respect to x, one can obtain the optimal value of the ratio, denoted hereinafter as $x_N^{(\mathrm{opt})}$. For small N, it has been obtained $x_N^{(\mathrm{opt})} = 1$ (for $N = 2, 3$), $\sqrt{3}$ ($N = 4$), and 2.016 ($N = 5$); see Ref. [22]. When $N \gg 1$, the optimal value of x is about $N/2$, for which $\mathcal{F}_{\mathrm{NOON}} \rightarrow \sqrt{8/9} \simeq 0.943$ (see Ref. [21] and Table I). In Fig. 1(c) we show the optimal value of the fidelity $\mathcal{F}_{\mathrm{NOON}}(x_N^{(\mathrm{opt})})$ as a function of N (the blue solid line), which coincides with Ref. [22]. From Eqs. (4) and (9),

TABLE I. For a given N, the fidelity $\mathcal{F}_{\text{NOON}}$ and the QFI $F_{Q,N}$ depend solely on the ratio $x \equiv |\alpha|^2/\tanh|\xi|$ and reach a maximum at $x_N^{(\text{opt})}$ and $x_N^{(\text{FI})}$, respectively. For $N = 2, 3$, $\mathcal{F}_{\text{NOON}} = F_{Q,N}/N^2 = 1$ at $x_N^{(\text{opt})} = x_N^{(\text{FI})} = 1$; while for $N = 4$, $\mathcal{F}_{\text{NOON}} = F_{Q,N}/N^2 = 0.933$ at $x_N^{(\text{opt})} = x_N^{(\text{FI})} = \sqrt{3}$.

N	5	6	7	8	9	10	100
$x_N^{(\text{opt})}, x_N^{(\text{FI})}$	2.016, 1.962	2.544, 2.488	2.961, 2.856	3.444, 3.323	3.908, 3.752	4.390, 4.213	49.405, 49.103
$\mathcal{F}_{\text{NOON}}, F_{Q,N}/N^2$	0.941, 0.945	0.924, 0.933	0.924, 0.938	0.920, 0.939	0.920, 0.943	0.920, 0.946	0.941, 0.995

one can also see that before the first beam splitter, $|\psi_N\rangle$ itself at $x = x_N^{(\text{opt})}$ approaches the NOON state $\exp(i\pi J_x/2)|\psi_{\text{NOON}}\rangle$, which shows the polarization along $\pm J_y$.

B. The Fisher information of the postselected N-photon state

We now investigate the CFI of the N-photon state in the photon-counting measurements and show that it always equals to the QFI under the PMC. To this end, we first calculate the QFI of the phase-encoded state $\exp(-i\varphi J_y)|\psi_N\rangle$, where the unitary operator represents sequent actions of the first beam splitter, the phase-shift accumulation in the path, and the second 50:50 beam splitter at the output ports, as illustrated in Fig. 1(a). Due to $\langle\psi_N|J_y|\psi_N\rangle = 0$, it is easy to obtain the QFI [10–14]:

$$F_{Q,N} = 4\langle\psi_N|J_y^2|\psi_N\rangle = 4\langle\psi_N^{\text{BS}}|J_z^2|\psi_N^{\text{BS}}\rangle = 4\sum_{\mu=-J}^{+J}\mu^2 p_\mu,$$
(10)

where $|\psi_N^{\text{BS}}\rangle$ denotes the N-photon state after the first beam splitter and its probability distribution $p_\mu(x)$ has been given by Eq. (6). Similar to the fidelity, one can see that the QFI depends on the ratio x and the number of photons N. For the cases $N = 2, 3,$ and 4, both of them reach maximum at $x_N^{(\text{opt})}$ because of the relation

$$F_{Q,N} = N^2\mathcal{F}_{\text{NOON}}(x) + 2(N-2)^2 p_{J-1}(x) + \cdots, \quad (11)$$

where $p_0(x)$, $p_{1/2}(x)$, and $p_1(x)$ are vanishing at $x = x_N^{(\text{opt})}$. When $N \geqslant 5$, however, $\{p_{|\mu|}(x)\}$ with $|\mu| < J$ provide nonvanishing contributions to the QFI. Numerically, we find that $F_{Q,N}$ reaches its maximum at $x_N^{(\text{FI})}$, which is slightly smaller than $x_N^{(\text{opt})}$ (see Table I). In Fig. 1(d) we plot the maximum of the QFI as a function of N and find $F_{Q,N} \gtrsim 0.933N^2$.

Next, we consider the photon-counting measurements over the phase-encoded state $\exp(-i\varphi J_y)|\psi_N\rangle$ and calculate the CFI. Again, we consider the PMC and rewrite the N-photon state as $|\psi_N\rangle = \exp(iN\theta_a)|\tilde{\psi}_N\rangle$, where $|\tilde{\psi}_N\rangle$ is given by Eq. (1) with $\theta_a = \theta_b = 0$. Note that the probability amplitudes of $|\tilde{\psi}_N\rangle$ and hence that of $\exp(-i\varphi J_y)|\tilde{\psi}_N\rangle$ are real, which result in the conditional probabilities (see Appendix A):

$$P_N(\mu|\varphi) = |\langle J,\mu|e^{-i\varphi J_y}|\psi_N\rangle|^2 = [\langle J,\mu|e^{-i\varphi J_y}|\tilde{\psi}_N\rangle]^2,$$
(12)

where $\mu = (N_1 - N_2)/2 \in [-J, +J]$ and $J = (N_1 + N_2)/2 = N/2$. Obviously, for a given N, there are $N + 1$ outcomes with their probabilities satisfying the normalization condition $\sum_\mu P_N(\mu|\varphi) = \langle\psi_N|\psi_N\rangle = 1$. Due to the real

probability amplitudes, $\langle J,\mu|\exp(-i\varphi J_y)|\tilde{\psi}_N\rangle \in \mathbb{R}$, we further obtain

$$\frac{\partial P_N(\mu|\varphi)}{\partial\varphi} = 2\sqrt{P_N(\mu|\varphi)}\langle J,\mu|(-iJ_y)\exp(-i\varphi J_y)|\tilde{\psi}_N\rangle \in \mathbb{R},$$

indicating that $\langle J,\mu|J_y\exp(-i\varphi J_y)|\tilde{\psi}_N\rangle$ is purely imaginary for each μ. This is the key point to obtain the CFI:

$$\begin{aligned}
F_N(\varphi) &= \sum_{\mu=-J}^{+J}\frac{[\partial P_N(\mu|\varphi)/\partial\varphi]^2}{P_N(\mu|\varphi)} \\
&= -4\sum_{\mu=-J}^{+J}[\langle J,\mu|J_y e^{-i\varphi J_y}|\tilde{\psi}_N\rangle]^2 \\
&= 4\langle\tilde{\psi}_N|J_y^2|\tilde{\psi}_N\rangle = F_{Q,N},
\end{aligned}$$
(13)

where $F_{Q,N}$ is the QFI of the phase-encoded state $\exp(-i\varphi J_y)|\psi_N\rangle$ under the PMC, given by Eq. (10).

As one of main results of this work, Eq. (13) indicates that as the "input" state, $|\psi_N\rangle$ at $x = x_N^{(\text{FI})}$ could provide a global phase estimation at the Heisenberg scaling [35], as $F_N(\varphi) = F_{Q,N} \gtrsim 0.933N^2$. However, this scaling is defined with respect to the number of photons being detected N. Furthermore, $|\psi_N\rangle$ is postselected by the N-photon detection events with the generation probability G_N, which is usually very small as $N \gg 1$ [see Fig. 2(a)]. Indeed, purely with the N-photon detection events (i.e., totally $N + 1$ outcomes with a definite N), one cannot improve the accuracy for estimating an unknown phase shift, since the CFI is weighted by the generation probability [30], i.e., $G_N F_N(\varphi)$. For the input $|\alpha\rangle_a \otimes |\xi\rangle_b$ with a given mean photon number $\bar{n} = |\alpha|^2 + \sinh^2|\xi|$, one can see that the weighted CFI for different values of N can reach only the classical limit $\sim O(\bar{n})$, as depicted by Fig. 2(c), where we considered the special case $\alpha, \xi \in \mathbb{R}$, for which the PMC is naturally fulfilled and therefore $F_N(\varphi) = F_{Q,N}$.

III. THE TOTAL FISHER INFORMATION

In order to improve the estimation precision, all the detection evens $\{N_1, N_2\}$ have to be taken into account in the photon-counting measurements, which gives ideal result of the CFI [10–14]:

$$F^{(\text{id})}(\varphi) = \sum_{2J=0}^{\infty}\sum_{\mu=-J}^{+J}\frac{[\partial P(J,\mu|\varphi)/\partial\varphi]^2}{P(J,\mu|\varphi)} = \sum_{N=0}^{\infty}G_N F_N(\varphi),$$
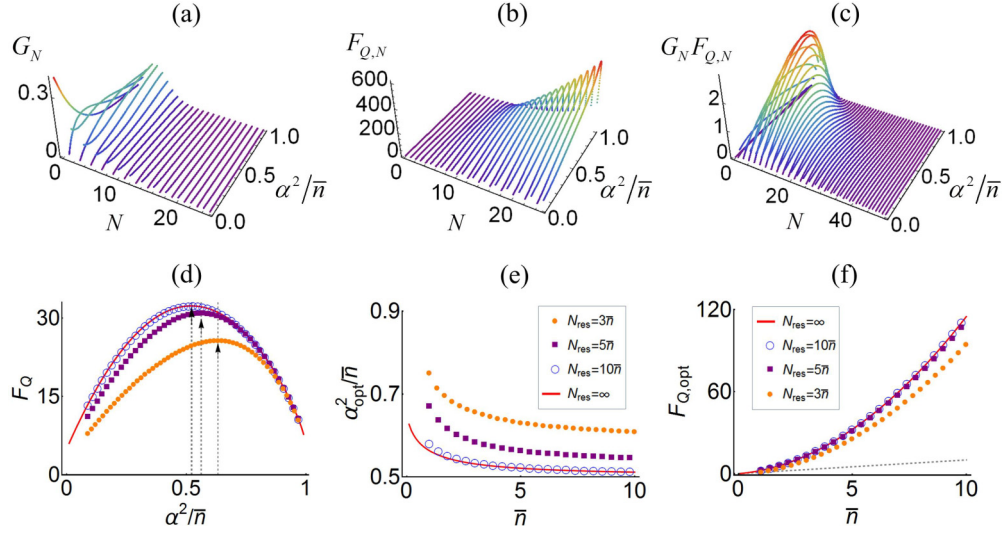(14)

FIG. 2. (a) The generation probability G_N, (b) the QFI of each N-photon state $F_{Q,N}$, (c) the weighted QFI $G_N F_{Q,N}$, and (d) the total QFI $F_Q(N_{res}, \bar{n}, \alpha^2)$, for $\bar{n} = 5$ fixed and $N_{res} = 3\bar{n}$ (solid circles), $5\bar{n}$ (squares), $10\bar{n}$ (open circles), and ∞ (red solid lines). The last case is given by Eq. (16), which predicts $\alpha_{opt}^2 \simeq \bar{n}/2$ and $F_{Q,opt}^{(id)} \simeq \bar{n}(\bar{n} + 3/2)$. For each a given $\bar{n} \in [1,10]$, using the same values of N_{res} and maximizing the total QFI with respect to α^2 to obtain (e) $\alpha_{opt}^2/\bar{n}$, and (f) the associated QFI $F_{Q,opt}$. In (c) the peak height of the weighted QFI is about $\bar{n}/2$. The vertical lines in (d) are the optimal value of α^2 for different values of N_{res}. The dashed line in (f) is the classical limit $F_Q = \bar{n}$.

where we have reexpressed the input state as $|\psi_{in}\rangle = \sum_N \sqrt{G_N} |\psi_N\rangle$, so we have

$$P(J, \mu | \varphi) \equiv |\langle J, \mu | e^{-i\varphi J_y} | \psi_{in} \rangle|^2 = G_N P_N(\mu | \varphi),$$

and $P_N(\mu|\varphi) \equiv |\langle J, \mu| \exp(-i\varphi J_y)|\psi_N\rangle|^2$, given by Eq. (12). Note that the total CFI is indeed a sum of each N-component contribution $F_N(\varphi)$ weighted by G_N. With only the N-photon detection events, the Fisher information is simply given by $G_N F_N(\varphi)$, as mentioned above.

Similar to Eq. (10), we further calculate the total QFI of the output state $\exp(-i\varphi J_y)|\psi_{in}\rangle$, which is independent from any specific measurement scheme and is given by $F_Q = 4(\langle J_y^2 \rangle_{in} - \langle J_y \rangle_{in}^2)$ [10–14]. For the input state $|\alpha\rangle_a \otimes |\xi\rangle_b$, we obtain $\langle J_y \rangle_{in} = 0$ and hence the ideal result of the QFI

$$F_Q^{(id)} = 4 \sum_{N=0}^{\infty} G_N \langle \psi_N | J_y^2 | \psi_N \rangle = \sum_{N=0}^{\infty} G_N F_{Q,N}, \quad (15)$$

where $F_{Q,N}$ is the QFI of the N-photon component. Under the PMC, we have show that for each N component $F_N(\varphi) = F_{Q,N}$, which naturally results in a global phase estimation $F^{(id)}(\varphi) = F_Q^{(id)}$ [35]. According to Refs. [15–17], one can obtain an explicit form of the QFI by directly calculating $4\langle J_y^2 \rangle_{in}$ (see also Appendix B):

$$F^{(id)}(\varphi) = F_Q^{(id)} = |\alpha|^2 e^{2|\xi|} + \sinh^2 |\xi|. \quad (16)$$

Given a constraint on the mean photon number $\bar{n}$, the maximum of the QFI was found to achieve the Heisenberg scaling $F_{Q,opt}^{(id)} \simeq \bar{n}(\bar{n} + 3/2) \sim O(\bar{n}^2)$ [16], provided $|\alpha|^2 \simeq \sinh^2|\xi| \simeq \bar{n}/2 \gg 1$ [15]; see also the red solid lines in Figs. 2(d)–2(f). However, such a scaling is possible only with exactly perfect photon-number-resolving detectors [18], which enable us to record an infinite number of the photon-counting events; see also Eq. (14).

Usually a single number-resolving detector can register only the number of photons up to four [19,20]. It is therefore important to investigate the CFI of each N component for N up to a finite number of photons being resolvable N_{res}. For brevity, we consider the input fields with the real amplitudes and large enough mean photon number (i.e., $\bar{n} = \alpha^2 + \sinh^2 \xi > 1$). Since the PMC is naturally fulfilled, the CFI is still a sum of each N component with the weight G_N and equals the QFI:

$$F_Q = 4 \sum_{N=0}^{N_{res}} G_N \langle \psi_N | J_y^2 | \psi_N \rangle = \sum_{N=0}^{N_{res}} G_N F_{Q,N}$$

$$= \sum_{N=0}^{N_{res}} \sum_{k=0}^{[N/2]} \left[N + 4k(N - 2k) + \frac{4k\alpha^2}{\tanh \xi} \right] [c_{N-2k}(0) s_{2k}(0)]^2,$$

$$(17)$$

where $|\psi_N\rangle$ is the N-photon state and $G_N = G_N(\alpha^2, \xi)$ denotes its generation probability, given by Eqs. (1) and (2). Obviously the QFI considered here depends on three variables $\{N_{res}, \alpha^2, \xi\}$, or equivalently, $\{N_{res}, \alpha^2, \bar{n}\}$ for a given $\bar{n}$. When $N_{res} \to \infty$, the ideal result of the QFI is recovered (see Appendix B).

The Heisenberg scaling of the QFI can be maintained for large enough N_{res}, provided that all the nonvanishing $\{G_N F_{Q,N}\}$ are included. To obtain the minimum value of N_{res}, we show G_N, $F_{Q,N}$, and $G_N F_{Q,N}$ against N and α^2 under a constraint on $\bar{n}$. From Fig. 2(b), one can see that $F_{Q,N}$ increases quadratically with N. This is because the QFI reaches its maximum $F_{Q,N} \sim O(N^2)$ when $\alpha^2/\tanh \xi = x_N^{(FI)}$ (see Table I), which corresponds to $\alpha^2/\bar{n} \to 1$, i.e., the classical light being dominant for a given $\bar{n} = \alpha^2 + \sinh^2 \xi$. On the other hand, the generation probability shows a little complex behavior on N; see Fig. 2(a). At $\alpha^2 = 0$, G_N is nonvanishing at even number of N and decreases monotonically with the increase of N. When $\alpha^2 \geqslant 1$ (i.e., $G_1 \geqslant G_0$), it reaches a

maximum at a certain value of N and then decreases. Similar to G_N, the weighted QFI $G_N F_{Q,N}$ reaches a maximum at $N \sim \bar{n}$ and then decreases with the increase of N. As depicted in Fig. 2(c), one can also see that the values of $G_N F_{Q,N}$ tend to vanishing as $N \gtrsim 5\bar{n}$, implying $N_{\text{res}} \sim 5\bar{n}$.

To confirm the above result, we maximize Eq. (17) with respect to α^2 for given $\bar{n}$ and N_{res}. Figure 2(d) shows F_Q as a function of α^2 for a fixed $\bar{n} = 5$, where $N_{\text{res}} = 3\bar{n}$ (the solid circles), $5\bar{n}$ (the squares), and $10\bar{n}$ (the open circles). When $N_{\text{res}} = \infty$ (the red solid line), the ideal result of the QFI is recovered and is given by Eq. (16), which reaches the Heisenberg scaling $\alpha^2_{\text{opt}} \simeq \bar{n}/2$ [15–17]. One can see that the QFI with $N_{\text{res}} = 10\bar{n}$ almost follows the ideal result. In Figs. 2(e) and 2(f), we show optimal value of the ratio $\alpha^2/\bar{n}$ and the associated QFI $F_{Q,\text{opt}} = F_Q(N_{\text{res}}, \bar{n}, \alpha^2_{\text{opt}})$ for each given value of $\bar{n} \in [1, 10]$, where we take the number resolution N_{res} as the same as Fig. 2(d). From Fig. 2(e), one can see that when $N_{\text{res}} > \bar{n}$, the optimal input state contains more coherent light photons than that of the squeezed vacuum. The Heisenberg scaling of the QFI is attainable with $N_{\text{res}} \gtrsim 5\bar{n}$, as depicted by Fig. 2(f).

Figure 3 shows $F_Q/F_{Q,\text{opt}}^{(\text{id})}$ as a function of $N_{\text{res}}/\bar{n}$ for the increase of $\bar{n}$ from 2 to 20. For each given $\bar{n}$, we first maximize the ideal QFI with respect to α^2 to obtain α^2_{opt} and $F_{Q,\text{opt}}^{(\text{id})}$, as depicted by the red lines of Figs. 2(d)–2(f), and then calculate the QFI of Eq. (17) using the same input state. Our numerical results show that $F_Q/F_{Q,\text{opt}}^{(\text{id})}$ increases with N_{res} and approaches 1 as $N_{\text{res}} \gg \bar{n}$.

To quantify how much phase information is kept by a finite cutoff N_{res}, we try to find an analytical result of $F_Q/F_{Q,\text{opt}}^{(\text{id})}$ in the limit $\bar{n} \to \infty$. To this end, we first separate the QFI into two terms $F_Q = F_Q^{(\text{id})} - F_Q^{(\text{lost})}$, where $F_Q^{(\text{lost})} = \sum_{N=N_{\text{res}}}^{\infty} G_N F_{Q,N}$ denotes the QFI being lost. This expression is the same to Eq. (17), except the sum over $N \in (N_{\text{res}}, \infty)$. Next, we note that the photon number distribution of the coherent state is much narrow than that of the squeezed vacuum, which enables us to obtain an approximate result of $F_Q^{(\text{lost})}$ (see Appendix B). Furthermore, the ideal result of the QFI can reach its maximum
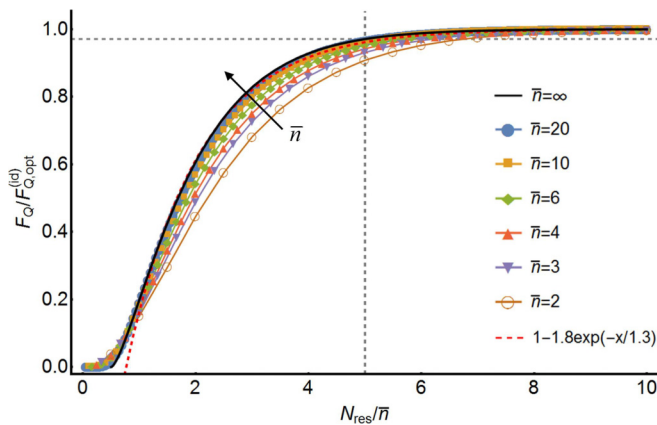

FIG. 3. Numerical results of $F_Q/F_{Q,\text{opt}}^{(\text{id})}$ as a function of $N_{\text{res}}/\bar{n}$ for given values of $\bar{n}$, using the optimal condition that maximizes Eq. (16). The solid line is given by our asymptotic result [Eq. (18)], and the dashed line is a fitting result for the case $\bar{n} = 20$. Both of them indicate that 96% of the ideal QFI can be obtained as long as $x = N_{\text{res}}/\bar{n} \gtrsim 5$ (the vertical dashed lines).

at the optimal condition $\alpha^2 = \sinh^2 \xi = \bar{n}/2 \gg 1$ [15–17]. Using the same input, we obtain

$$\frac{F_Q}{F_{Q,\text{opt}}^{(\text{id})}} \approx 1 - \lim_{\bar{n}\to\infty} \frac{F_Q^{(\text{lost})}(x,\bar{n})}{\bar{n}(\bar{n}+3/2)}$$

$$\approx \text{erf}(\sqrt{x-1/2}) - \frac{2e^{-x+1/2}}{\sqrt{\pi}}\sqrt{x-1/2}, \quad (18)$$

where $x \equiv N_{\text{res}}/\bar{n}$ and $\text{erf}(\cdots)$ denotes the error function. Our analytical result shows a good agreement with the numerical results; see the solid lines in Fig. 3. When $N_{\text{res}} \gtrsim 5\bar{n}$, it predicts that over 96% of the ideal QFI can be kept, while for $N_{\text{res}} < \bar{n}/2$, most of the phase information is lost.

Finally, it should be mentioned that coherent-state interferometry has been demonstrated using two visible light photon counters with $N_{\text{res}} = 8$ [19]. This number resolution is large enough to realize the global phase estimation for the coherent-state input $\bar{n} \simeq 1$. Based upon a Bayesian protocol [19], the achievable phase sensitivity was found almost saturating a quantum Cramér-Rao bound over a wide phase interval, in agreement with the theoretical prediction $F(\varphi) = F_Q = \bar{n}$. To realize higher-precision optical metrology, it requires a bright nonclassical light source with larger mean photon number [15], low photon loss [14,36–38], and low noise [39–50], as well as the photon counters with high detection efficiency [51] and large enough number resolution.

IV. CONCLUSION

In summary, we have investigated optical phase estimation with coherent $\otimes$ squeezed vacuum light by using imperfect photon counters with an upper threshold N_{res} for the photon number resolution. We show that both the CFI and the QFI are the sum of the contributions from individual N-photon components, and the CFI always saturates the QFI for each individual N-photon component. For ideal photon-counting detectors with $N_{\text{res}} \to \infty$, the CFI or the QFI attains its maximum $F_{Q,\text{opt}}^{(\text{id})} \sim \bar{n}^2$ when $|\alpha|^2 \simeq \sinh^2|\xi|$, leading to the Heisenberg limit of the estimation precision. For the detectors with large enough number resolution $N_{\text{res}} > \bar{n}$, we find that the optimal input state contains more coherent light photons than that of the squeezed vacuum. We present an analytical result that quantifies the amount of lost information and show that over 96% of an ideal QFI can be attained as long as $N_{\text{res}} \gtrsim 5\bar{n}$, while for $N_{\text{res}} < \bar{n}/2$, most of the phase information is lost. Our results highlight the important influence of the finite number resolution of photon-counting detectors for optical phase estimation. It is also interesting to explore the performance of other continuous-variable input states, e.g., a product of two squeezed vacuum $|\xi\rangle \otimes |-\xi\rangle$ [52], when realistic photon counters are used.

ACKNOWLEDGMENTS

APPENDIX A: THE N-PHOTON STATE UNDER THE PHASE-MATCHING CONDITION

Formally, a single-mode squeezed vacuum of light is defined by $|\xi\rangle = S(\xi)|0\rangle$, with the squeeze operator [53–55]:

$$
\begin{aligned}
S(\xi) &= \exp\left[\frac{1}{2}(\xi^* b^2 - \xi b^{\dagger 2})\right] \\
&= \exp\left(-e^{i\theta_b}\frac{\tanh|\xi|}{2}b^{\dagger 2}\right)\left(\frac{1}{\cosh|\xi|}\right)^{b^\dagger b + \frac{1}{2}} \\
&\quad \times \exp\left(e^{-i\theta_b}\frac{\tanh|\xi|}{2}b^2\right),
\end{aligned}
\tag{A1}
$$

where $\xi = |\xi|\exp(i\theta_b)$ denotes the complex amplitude of the squeezed vacuum. In the Fock basis, using $b|0\rangle = 0$, the squeezed vacuum can be expressed as

$$
|\xi\rangle = \frac{1}{\sqrt{\cosh|\xi|}}\exp\left(-e^{i\theta_b}\frac{\tanh|\xi|}{2}b^{\dagger 2}\right)|0\rangle = \sum_{k=0}^{+\infty}s_{2k}|2k\rangle,
\tag{A2}
$$

where $s_{2k} \equiv \langle 2k|\xi\rangle$ denote the probability amplitudes of the squeezed vacuum, given by

$$
\begin{aligned}
s_{2k}(\theta_b) &= \frac{\sqrt{(2k)!}}{k!\sqrt{\cosh|\xi|}}\left(-e^{i\theta_b}\frac{\tanh|\xi|}{2}\right)^k, \\
\text{or} \quad s_k(\theta_b) &= \frac{H_k(0)}{\sqrt{k!\cosh|\xi|}}\left(e^{i\theta_b}\frac{\tanh|\xi|}{2}\right)^{k/2},
\end{aligned}
\tag{A3}
$$

with the Hermite polynomials $H_{2n}(0) = (-1)^n(2n)!/n!$ and $H_{2n+1}(0) = 0$.

Note that one can obtain an explicit form of the squeezed vacuum using the disentangling formula [53–55], as done in Eq. (A1), or, alternatively, directly solving the eigenvalue equation $S(\xi)b|0\rangle = S(\xi)bS^\dagger(\xi)|\xi\rangle = 0$ [56]. The single-mode squeezed vacuum contains only an even number of photons and has been generated in experiments [57–63].

We now consider the interferometer fed with the squeezed vacuum from one input port and a coherent-state light from another port. The coherent state is given by $|\alpha\rangle = \sum_n c_n(\theta_a)|n\rangle$, with the probability amplitudes

$$
c_n(\theta_a) \equiv \langle n|\alpha\rangle = e^{-|\alpha|^2/2}\frac{|\alpha|^n e^{in\theta_a}}{\sqrt{n!}},
\tag{A4}
$$

where $\alpha = |\alpha|\exp(i\theta_a)$ denotes the complex amplitude of the coherent light. In Eqs. (A3) and (A4), we have written explicitly the phase dependence of the probability amplitudes, purely for later use.

Under the phase-matching condition (PMC): $\cos(\theta_b - 2\theta_a) = +1$, we now calculate the probability amplitudes of the N-photon states $|\psi_N\rangle$ as

$$
\begin{aligned}
&\frac{c_{N-2k}(\theta_a)s_{2k}(\theta_b)}{\sqrt{G_N}} \\
&= (-1)^k\frac{e^{iN\theta_a}e^{ik(\theta_b-2\theta_a)}}{\sqrt{R_N(x)}}\frac{\sqrt{(2k)!}}{k!\sqrt{(N-2k)!}}(2x)^{(N-2k)/2}
\end{aligned}
$$

$$
\begin{aligned}
&\xrightarrow{\text{PMC}} (-1)^k\frac{e^{iN\theta_a}}{\sqrt{R_N(x)}}\frac{\sqrt{(2k)!}}{k!\sqrt{(N-2k)!}}(2x)^{(N-2k)/2} \\
&\equiv e^{iN\theta_a}\frac{c_{N-2k}(0)s_{2k}(0)}{\sqrt{G_N}},
\end{aligned}
\tag{A5}
$$

where we have used an explicit form of G_N, given by Eq. (2), and the condition $\exp[ik(\theta_b - 2\theta_a)] = +1$ for integers k. Note that Eq. (1) can be rewritten as $|\psi_N\rangle = \exp(iN\theta_a)|\tilde{\psi}_N\rangle$, where $|\tilde{\psi}_N\rangle$ denotes the N-photon states with real amplitudes (i.e., $\theta_a = \theta_b = 0$).

Finally, we consider a unitary operation $\exp(-i\varphi J_\eta)$ on the N-photon states $|\psi_N\rangle$, with $J_\eta = J_x\cos\eta + J_y\sin\eta$, to obtain Eqs. (5) and (6). Under the PMC, we obtain

$$
\begin{aligned}
e^{-i\varphi J_\eta}|\psi_N\rangle &= e^{iN\theta_a}e^{-i\varphi J_\eta}|\tilde{\psi}_N\rangle = e^{iN\theta_a}e^{-i\eta J_z}e^{-i\varphi J_x}e^{i\eta J_z}|\tilde{\psi}_N\rangle \\
&= \frac{e^{iN\theta_a}}{\sqrt{G_N}}e^{-i\eta J_z}e^{-i\varphi J_x} \\
&\quad \times \sum_{k=0}^{[N/2]}e^{i\eta(J-2k)}c_{N-2k}(0)s_{2k}(0)|J,J-2k\rangle,
\end{aligned}
\tag{A6}
$$

where, in the second step, we have used the relation $\exp(-i\eta J_z)f(J_x)\exp(i\eta J_z) = f(J_\eta)$, and Eq. (1) with $\theta_a = \theta_b = 0$ for $|\tilde{\psi}_N\rangle$, which is expressed in terms of the states $|J,J-2k\rangle = |N-2k\rangle_a \otimes |2k\rangle_b$. In the eigenbasis of J_z, we obtain the probability amplitudes

$$
\begin{aligned}
\langle J,\mu|e^{-i\varphi J_\eta}|\psi_N\rangle &= \frac{e^{iN\theta_a}}{\sqrt{G_N}}e^{-i\eta\mu}\sum_{k=0}^{[N/2]}e^{i\eta(J-2k)}c_{N-2k}(0)s_{2k}(0) \\
&\quad \times \langle J,\mu|e^{-i\varphi J_x}|J,J-2k\rangle \\
&= \frac{e^{iN\theta_a}}{\sqrt{R_N(x)}}e^{i(\frac{\pi}{2}-\eta)(\mu-J)}\sum_{k=0}^{[N/2]}e^{-i2k\eta} \\
&\quad \times \frac{\sqrt{(2k)!}}{k!\sqrt{(N-2k)!}}(2x)^{N/2-k}d_{\mu,J-2k}^J(\varphi),
\end{aligned}
\tag{A7}
$$

where, in the last step, we have introduced Wigner's d-matrix $d_{\mu,\nu}^J(\varphi)$. Obviously, for the special case $\eta = 0$ and $\varphi = \pi/2$, we obtain the N-photon state after the first 50:50 beam splitter $\exp(-i\pi J_x/2)|\psi_N\rangle$ and its probability distributions; see Eqs. (5) and (6). For $\eta = \pi/2$ and arbitrary φ, we can obtain the output state $\exp(-i\varphi J_y)|\psi_N\rangle$ and its probabilities $P_N(\mu|\varphi)$.

APPENDIX B: ANALYTICAL RESULTS OF THE QUANTUM FISHER INFORMATION

In a lossless and noiseless interferometer, the QFI of a pure phase-encoded state $|\psi_{\text{out}}\rangle = \exp(-i\varphi G)|\psi_{\text{in}}\rangle$ is simply given by $F_Q = 4(\langle G^2\rangle_{\text{in}} - \langle G\rangle_{\text{in}}^2)$ [10–14], where G is a Hermitian operator. For the squeezed-state interferometer, as illustrated in Fig. 1(a), the input state is the product of a coherent state and a squeezed vacuum, i.e., $|\psi_{\text{in}}\rangle = |\alpha\rangle_a \otimes |\xi\rangle_b$, and the phase shifter is given by $G = J_x$, or J_y, where, for brevity, we have introduced the angular-momentum operators $J_+ = (J_-)^\dagger = a^\dagger b$ and $J_z = (a^\dagger a - b^\dagger b)/2$, with the bosonic operators of two light fields a and b.

According to Ref. [15], the QFI of the output state $\exp(-i\varphi J_y)|\psi_{\text{in}}\rangle$ is optimal when the two injected light fields are phase matched, i.e., the PMC $\cos(\theta_b - 2\theta_a) = +1$. Recently Liu *et al.* [17] have derived a more general form of the PMC for the interferometer $U_{\text{MZI}}(\varphi) = \exp(-i\varphi J_y)$, where a superposition of even or odd number of photons is injected from one port and an arbitrary state from another port.

To show it clearly, we focus on the PMC $\cos(\theta_b - 2\theta_a) = +1$ and calculate the QFI of $\exp(-i\varphi J_y)|\psi_{\text{in}}\rangle$,

$$F_Q^{(\text{id})} = 4\langle J_y^2\rangle_{\text{in}}$$

$$= \langle (a^\dagger a + b^\dagger b + 2a^\dagger a b^\dagger b) - (a^{\dagger 2}b^2 + \text{H.c.})\rangle_{\text{in}}, \quad (\text{B1})$$

where H.c. denotes the Hermitian conjugate. There are two contributions to the QFI. First, it is easy to obtain

$$\langle (a^\dagger a + b^\dagger b + 2a^\dagger a b^\dagger b)\rangle_{\text{in}} = \bar{n}_a + \bar{n}_b + 2\bar{n}_a\bar{n}_b, \quad (\text{B2})$$

with $\bar{n}_a = |\alpha|^2$ and $\bar{n}_b = \sinh^2|\xi|$ being the mean photon number of light fields from two input ports. Second, using the relation $S^\dagger(\xi)bS(\xi) = b\cosh|\xi| - b^\dagger e^{i\theta_b}\sinh|\xi|$, we obtain

$$\langle a^{\dagger 2}b^2\rangle_{\text{in}} = \alpha^{*2}\langle \xi|b^2|\xi\rangle = -\bar{n}_a\sqrt{\bar{n}_b(1+\bar{n}_b)}e^{i(\theta_b - 2\theta_a)}. \quad (\text{B3})$$

Therefore, the ideal result of the QFI is given by

$$F_Q^{(\text{id})} = \bar{n}_a[1 + 2\bar{n}_b + 2\sqrt{\bar{n}_b(1+\bar{n}_b)}\cos(\theta_b - 2\theta_a)] + \bar{n}_b \leqslant \bar{n}_a[1 + 2\bar{n}_b + 2\sqrt{\bar{n}_b(1+\bar{n}_b)}] + \bar{n}_b, \quad (\text{B4})$$

where the equality holds when the PMC is fulfilled: $\cos(\theta_b - 2\theta_a) = +1$. Similarly, one can note that the PMC $\cos(\theta_b - 2\theta_a) = -1$ is a good choice for the output state $\exp(-i\varphi J_x)|\alpha\rangle_a \otimes |\xi\rangle_b$, e.g., the phases of the two light fields $(\theta_a, \theta_b) = (0, \pi)$ [21] and $(\pi/2, 0)$ [22]. Furthermore, one can simplify the ideal result of the QFI as Eq. (16), using the relation $1 + 2\bar{n}_b + 2\sqrt{\bar{n}_b(1+\bar{n}_b)} = e^{2|\xi|}$.

With a finite number resolution N_{res}, we have shown that the CFI and the QFI are the same and given by Eqs. (17), which can be rewritten as

$$F_Q = \sum_{N_a=0}^{N_{\text{res}}} \sum_{N_b=0}^{N_{\text{res}}-N_a} \left[N_a + \left(1 + 2N_a + \frac{2\alpha^2}{\tanh\xi}\right)N_b\right]\left[c_{N_a}(0)s_{N_b}(0)\right]^2$$

$$\approx \bar{n}_a \sum_{N_b=0}^{N_{\text{res}}-\bar{n}_a} \left[s_{N_b}(0)\right]^2 + \left(1 + 2\bar{n}_a + \frac{2\bar{n}_a}{\tanh\xi}\right)\sum_{N_b=0}^{N_{\text{res}}-\bar{n}_a} N_b\left[s_{N_b}(0)\right]^2, \quad (\text{B5})$$

where, for brevity, we consider the two light fields with real amplitudes, i.e., $\theta_b = \theta_a = 0$, and the probability amplitudes $c_n(0)$ and $s_k(0)$ are given by Eqs. (A3) and (A4). In the above result, we made an approximation

$$\sum_{N_a=0}^{N_{\text{res}}} \sum_{N_b=0}^{N_{\text{res}}-N_a} f(N_a)g(N_b)\left[c_{N_a}(0)s_{N_b}(0)\right]^2 \approx \sum_{N_a=0}^{\infty} f(N_a)\left[c_{N_a}(0)\right]^2 \sum_{N_b=0}^{N_{\text{res}}-\bar{n}_a} g(N_b)\left[s_{N_b}(0)\right]^2, \quad (\text{B6})$$

where $\bar{n}_a = |\alpha|^2$ and the sum over the mode b is still kept, since the photon number distribution of the squeezed vacuum is usually wider than that of the coherent state (even for $\bar{n}_b < \bar{n}_a$) [56,61]. For a finite $\bar{n}_a$ and $N_{\text{res}} \to \infty$, it is easy to obtain the ideal result of the QFI as

$$F_Q \approx \bar{n}_a + \left(1 + 2\bar{n}_a + \frac{2\bar{n}_a}{\tanh\xi}\right)\bar{n}_b = F_Q^{(\text{id})}, \quad (\text{B7})$$

where $\tanh\xi = \sqrt{\bar{n}_b/(\bar{n}_b + 1)}$ and $F_Q^{(\text{id})}$ is given by Eq. (B4).

Finally, we consider a finite number resolution with large enough N_{res} ($>\bar{n}_a$), and derive analytical result of the QFI. To this end, we first rewrite Eq. (B5) as $F_Q = F_Q^{(\text{id})} - F_Q^{(\text{lost})}$, where $F_Q^{(\text{lost})}$ quantifies the lost phase information caused by the finite number resolution, given by

$$F_Q^{(\text{lost})} = 4\sum_{N=N_{\text{res}}}^{\infty} G_N\langle\psi_N|J_y^2|\psi_N\rangle \approx \bar{n}_a \sum_{k=N_{\text{res}}-\bar{n}_a}^{\infty} [s_k(0)]^2 + \left(1 + 2\bar{n}_a + \frac{2\bar{n}_a}{\tanh\xi}\right)\sum_{k=N_{\text{res}}-\bar{n}_a}^{\infty} k[s_k(0)]^2$$

$$\approx \left(2\bar{n}_a + \frac{2\bar{n}_a}{\tanh\xi}\right)\int_{N_{\text{res}}-\bar{n}_a}^{\infty} k\,dk\,\frac{(\tanh\xi)^k}{\sqrt{2\pi k}\cosh\xi}, \quad (\text{B8})$$

where, in the last step, we keep only the terms $\sim O(\bar{n}^2)$. In addition, we replace the sum over k by an integral and use Stirling's formula $k! \approx \sqrt{2k\pi}(k/e)^k$. When $N_{\text{res}} \leqslant \bar{n}_a$, it is easy to find $F_Q^{(\text{lost})} \approx F_Q^{(\text{id})}$ and hence the achievable QFI $F_Q \sim O(\bar{n}^0)$ or $O(\bar{n}^1)$, corresponding to an almost complete loss of the phase information or the ultimate estimation precision in the classical limit. To enlarge the QFI, we take $N_{\text{res}} > \bar{n}_a$ and obtain

$$F_Q^{(\text{lost})} \approx \frac{2\bar{n}_a\bar{n}_b}{B^{3/2}}(1 + e^{-\frac{B}{2\bar{n}_b}})\left[\text{erfc}\left(\sqrt{\frac{N_{\text{res}}-\bar{n}_a}{2\bar{n}_b}}B\right) + \frac{2}{\sqrt{\pi}}e^{-\frac{N_{\text{res}}-\bar{n}_a}{2\bar{n}_b}B}\sqrt{\frac{N_{\text{res}}-\bar{n}_a}{2\bar{n}_b}}B\right], \quad (\text{B9})$$

where $\bar{n}_b = \sinh^2 \xi$, $B(\bar{n}_b) = \bar{n}_b \log[(1 + \bar{n}_b)/\bar{n}_b]$, and $\mathrm{erfc}(x) = 1 - \mathrm{erf}(x)$ denotes the complementary error function. Our analytical result coincides with the numerical results in Figs. 2(d)–2(f). In the limit $\bar{n}_a = \bar{n}_b = \bar{n}/2 \to \infty$, we obtain $B(\bar{n}_b) \to 1$ and hence

$$F_Q^{(\mathrm{lost})} \approx \bar{n}^2 \left[\mathrm{erfc}(\sqrt{x - 1/2}) + \frac{2e^{-(x-1/2)}}{\sqrt{\pi}} \sqrt{(x - 1/2)} \right], \tag{B10}$$

where $x \equiv N_{\mathrm{res}}/\bar{n} > 1/2$. This result gives Eq. (18).

[1] C. M. Caves, Phys. Rev. D **23**, 1693 (1981).

[2] V. Giovannetti, S. Lloyd, and L. Maccone, Nat. Photonics **5**, 222 (2011).

[3] J. Ma, X. Wang, C. P. Sun, and F. Nori, Phys. Rep. **509**, 89 (2011).

[4] J. Aasi *et al.*, Nat. Photonics **7**, 613 (2013).

[5] J. P. Dowling and K. P. Seshadreesan, J. Lightwave Techn. **33**, 2359 (2015); J. P. Dowling, Contemp. Phys. **49**, 125 (2008).

[6] J. C. F. Matthews, X. Q. Zhou, H. Cable, P. J. Shadbolt, D. J. Saunders, G. A. Durkin, G. J. Pryde, and J. L. O'Brien, NPJ Quantum Inf. **2**, 16023 (2016).

[7] L. Pezzé, A. Smerzi, M. K. Oberthaler, R. Schmied, and P. Treutlein, arXiv:1609.01609 [quant-ph].

[8] C. W. Helstrom, *Quantum Detection and Estimation Theory* (Academic, New York, 1976).

[9] S. M. Kay, *Fundamentals of Statistical Signal Processing: Estimation Theory* (Prentice-Hall, Englewood Cliffs, NJ, 1993).

[10] S. L. Braunstein and C. M. Caves, Phys. Rev. Lett. **72**, 3439 (1994).

[11] S. L. Braunstein, C. M. Caves, and G. J. Milburn, Ann. Phys. (N.Y.) **247**, 135 (1996).

[12] S. Luo, Phys. Rev. Lett. **91**, 180403 (2003).

[13] L. Pezzé and A. Smerzi, Phys. Rev. Lett. **102**, 100401 (2009); F. Benatti, R. Floreanini, and U. Marzolino, Ann. Phys. **325**, 924 (2010).

[14] R. Demkowicz-Dobrzański, U. Dorner, B. J. Smith, J. S. Lundeen, W. Wasilewski, K. Banaszek, and I. A. Walmsley, Phys. Rev. A **80**, 013825 (2009); U. Dorner, R. Demkowicz-Dobrzański, B. J. Smith, J. S. Lundeen, W. Wasilewski, K. Banaszek, and I. A. Walmsley, Phys. Rev. Lett. **102**, 040403 (2009).

[15] L. Pezzé and A. Smerzi, Phys. Rev. Lett. **100**, 073601 (2008).

[16] M. D. Lang and C. M. Caves, Phys. Rev. Lett. **111**, 173601 (2013).

[17] J. Liu, X. Jing, and X. Wang, Phys. Rev. A **88**, 042316 (2013).

[18] K. P. Seshadreesan, P. M. Anisimov, H. Lee, and J. P. Dowling, New J. Phys. **13**, 083026 (2011).

[19] L. Pezzé, A. Smerzi, G. Khoury, J. F. Hodelin, and D. Bouwmeester, Phys. Rev. Lett. **99**, 223602 (2007).

[20] B. E. Kardynal, Z. L. Yuan, and A. J. Shields, Nat. Photonics **2**, 425 (2008).

[21] H. F. Hofmann and T. Ono, Phys. Rev. A **76**, 031806(R) (2007); T. Ono and H. F. Hofmann, *ibid.* **81**, 033819 (2010).

[22] I. Afek, O. Ambar, and Y. Silberberg, Science **328**, 879 (2010).

[23] P. Kok, H. Lee, and J. P. Dowling, Phys. Rev. A **65**, 052104 (2002).

[24] G. J. Pryde and A. G. White, Phys. Rev. A **68**, 052315 (2003).

[25] A. N. Boto, P. Kok, D. S. Abrams, S. L. Braunstein, C. P. Williams, and J. P. Dowling, Phys. Rev. Lett. **85**, 2733 (2000).

[26] M. W. Mitchell, J. S. Lundeen, and A. M. Steinberg, Nature (London) **429**, 161 (2004).

[27] P. Walther, J.-W. Pan, M. Aspelmeyer, R. Ursin, S. Gasparoni, and A. Zeilinger, Nature (London) **429**, 158 (2004).

[28] H. Cable and J. P. Dowling, Phys. Rev. Lett. **99**, 163604 (2007).

[29] F. Töppel, M. V. Chekhova, and G. Leuchs, arXiv:1607.01296.

[30] J. Combes, C. Ferrie, Z. Jiang, and C. M. Caves, Phys. Rev. A **89**, 052117 (2014).

[31] S. Pang and T. A. Brun, Phys. Rev. Lett. **115**, 120401 (2015).

[32] S. A. Haine, S. S. Szigeti, M. D. Lang, and C. M. Caves, Phys. Rev. A **91**, 041802 (2015).

[33] N. Tajima, Phys. Rev. C **91**, 014320 (2015).

[34] X. M. Feng, P. Wang, W. Yang, and G. R. Jin, Phys. Rev. E **92**, 043307 (2015).

[35] H. F. Hofmann, Phys. Rev. A **79**, 033822 (2009).

[36] J. Joo, W. J. Munro, and T. P. Spiller, Phys. Rev. Lett. **107**, 083601 (2011).

[37] Y. M. Zhang, X. W. Li, W. Yang, and G. R. Jin, Phys. Rev. A **88**, 043832 (2013).

[38] P. A. Knott, W. J. Munro, and J. A. Dunningham, Phys. Rev. A **89**, 053812 (2014).

[39] A. Al-Qasimi and D. F. V. James, Opt. Lett. **34**, 268 (2009).

[40] B. Teklu, M. G. Genoni, S. Olivares, and M. G. A. Paris, Phys. Scr. **T140**, 014062 (2010).

[41] Y. C. Liu, G. R. Jin, and L. You, Phys. Rev. A **82**, 045601 (2010).

[42] D. Brivio, S. Cialdi, S. Vezzoli, B. T. Gebrehiwot, M. G. Genoni, S. Olivares, and M. G. A. Paris, Phys. Rev. A **81**, 012305 (2010).

[43] M. G. Genoni, S. Olivares, and M. G. A. Paris, Phys. Rev. Lett. **106**, 153603 (2011).

[44] M. G. Genoni, S. Olivares, D. Brivio, S. Cialdi, D. Cipriani, A. Santamato, S. Vezzoli, and M. G. A. Paris, Phys. Rev. A **85**, 043817 (2012).

[45] B. M. Escher, L. Davidovich, N. Zagury, and R. L. de Matos Filho, Phys. Rev. Lett. **109**, 190404 (2012).

[46] W. Zhong, Z. Sun, J. Ma, X. Wang, and F. Nori, Phys. Rev. A **87**, 022337 (2013).

[47] B. Roy Bardhan, K. Jiang, and J. P. Dowling, Phys. Rev. A **88**, 023857 (2013).

[48] X. M. Feng, G. R. Jin, and W. Yang, Phys. Rev. A **90**, 013807 (2014).

[49] M. Zwierz and H. M. Wiseman, Phys. Rev. A **89**, 022107 (2014).

[50] Y. Gao and R. M. Wang, Phys. Rev. A **93**, 013809 (2016).

[51] B. Calkins, P. L. Mennea, A. E. Lita, B. J. Metcalf, W. S. Kolthammer, A. Lamas-Linares, J. B. Spring, P. C. Humphreys, R. P. Mirin, J. C. Gates, P. G. R. Smith, I. A. Walmsley, T. Gerrits, and S. W. Nam, Opt. Express **21**, 22657 (2013).

[52] M. D. Lang and C. M. Caves, Phys. Rev. A **90**, 025802 (2014).

[53] R. A. Fisher, M. M. Nieto, and V. D. Sandberg, Phys. Rev. D **29**, 1107 (1984).

[54] D. R. Truax, Phys. Rev. D **31**, 1988 (1985).

[55] M. Ban, J. Opt. Soc. Am. B **10**, 1347 (1993).

[56] C. C. Gerry and P. L. Knight, *Introductory Quantum Optics* (Cambridge University Press, Cambridge, 2005).

[57] R. E. Slusher, L. W. Hollberg, B. Yurke, J. C. Mertz, and J. F. Valley, Phys. Rev. Lett. **55**, 2409 (1985).

[58] L.-A. Wu, H. J. Kimble, J. L. Hall, and H. Wu, Phys. Rev. Lett. **57**, 2520 (1986).

[59] L.-A. Wu, M. Xiao, and H. J. Kimble, J. Opt. Soc. Am. B **4**, 1465 (1987).

[60] R. E. Slusher, P. Grangier, A. LaPorta, B. Yurke, and M. J. Potasek, Phys. Rev. Lett. **59**, 2566 (1987).

[61] G. Breitenbach, S. Schiller, and J. Mlynek, Nature (London) **387**, 471 (1997).

[62] H. Vahlbruch, M. Mehmet, S. Chelkowski, B. Hage, A. Franzen, N. Lastzka, S. Goßler, K. Danzmann, and R. Schnabel, Phys. Rev. Lett. **100**, 033602 (2008).

[63] H. Vahlbruch, M. Mehmet, K. Danzmann, and R. Schnabel, Phys. Rev. Lett. **117**, 110801 (2016).